Journal of Intelligent Transportation Systems, 14(2):95–108, 2010

ISSN: 1547-2450 print / 1547-2442 online
DOI: 10.1080/15472451003719756

Optimization of Control Parameters for Adaptive Traffic-Actuated Signal Control

XING ZHENG,[1] WILL RECKER,[1] and LIANYU CHU[2]

[1]Institute of Transportation Studies, University of California, Irvine, Irvine, California, USA
[2]California Center for Innovative Transportation, University of California, Berkeley, Berkeley, California, USA

The authors propose a real-time adaptive signal control model that aims to maintain the adaptive functionality of actuated controllers while improving the performance of traffic-actuated control systems. In this model, a flow-prediction algorithm is formulated to estimate the future vehicle arrival flow for each signal phase at the target intersection on the basis of the available signal-timing data obtained from previous control cycles. Optimal timing parameters are determined on the basis of these estimations and are used as signal-timing data for further optimizations. To be consistent with the operation logic of existing signal-control devices, this model is developed to optimize the basic control parameters that can be found in modern actuated controllers. Microscopic simulation is used to test and evaluate the proposed control model in a calibrated network consisting of 38 actuated signals. Simulation results indicate that this model has the potential to improve the performance of the signalized network under different traffic conditions.

Keywords adaptive signal control; microscopic simulation; optimization

INTRODUCTION

At a signalized intersection, traffic signals typically operate in one of two different control modes—either pretimed or actuated (semi-actuated and full-actuated). In *pretimed control*, all of the control parameters—including cycle length, phase splits, and phase sequence—are preset offline on the basis of an assumed deterministic demand level at different time periods of day. This control mode has a limited ability to accommodate the traffic fluctuations that are commonly found in urban networks. In *actuated control*, the cycle length, phase splits, and even phase sequence can be changed in response to the real-time vehicle actuations registered at detectors or other at traffic sensors, but these changes are still subject to a set of predefined, fixed control parameters (e.g., minimum green, unit extension, maximum green) that are not accordingly responsive to the varying traffic condition. Alternatively, an online adaptive control that determines real-time signal operation parameters offers a potential solution to the aforementioned problem.

Address correspondence to Xing Zheng, Institute of Transportation Studies, University of California, Irvine, 4000 AIR Building, Irvine, CA 92697, USA. E-mail: xzheng1@uci.edu

Existing adaptive control systems that have been deployed, such as SCOOT (Hunt, Robertson, Bretherton, and Winton, 1981; Robertson and Bretherton, 1991) and SCATS (Lowrie, 1992; Sims and Dobinson, 1980), which are considered to be *online* algorithms, adjust timing parameters incrementally to accommodate the changing traffic demands. This control strategy is, in fact, to pick a best preset timing plan, on the basis of the detector data, to match current traffic conditions. The major drawback of these systems is that they are not proactive and thus cannot satisfy significant transients effectively. RHODES (Mirchandani and Head, 2001), a real-time traffic-adaptive control system developed at the University of Arizona, uses a traffic flow arrival algorithm—PREDICT (Head, 1995)—to improve effectiveness when calculating online phase timings. In the PREDICT algorithm, detector information on approaches of every upstream intersection, together with the traffic state and control plan of upstream signals, are used to predict future traffic volumes. However, it assumes that all surrounding upstream intersections have fixed-time signalized planning, an assumption that is violated in virtually every modern system.

In none of these previous systems do the embedded traffic flow prediction models fully use available detector information and control features. Consequently, their applicability is

confined only to particular factors and thus restricted in achieving comprehensively good performance. Also, although a number of theoretical issues involving truly adaptive systems have been explored and proposed (e.g., Lin and Wang, 2004; Wong and Wong, 2003), their applicability to a functional model capable of addressing real-world situations has not been tested.

For any traffic-actuated control system, at least three data resources—current phase state, signal-timing plan, and detector output—can be exploited to infer a relatively rich body of information that can be used in adapting the operation of a controller to the current, or expected, traffic condition. In the work reported in this article, we introduce a real-time adaptive control model that aims to maintain the adaptive functionality of actuated controllers while improving the performance of traffic-actuated control systems. This model incorporates a traffic flow prediction algorithm that sufficiently uses the available signal-timing data gleaned from previous control cycles to estimate the future vehicle arrival flow for each actuated phase. Optimal timing parameters are determined on the basis of these estimations and are used as signal-timing data for further optimizations. This online, dynamic computation process properly reflects the functionality of truly adaptive controllers. Particularly noteworthy here is that the proposed model is developed to provide an adaptive control strategy for existing actuated signal-control systems. Coordinated operation and any other adaptive control are not considered in this article.

We describe the methodology underlying the proposed adaptive control model in detail in the following section. Then, microscopic simulation is used to test and evaluate the performance of this model in a calibrated network. Last, we present conclusions and potential future work.

METHOD

Overview

The proposed adaptive control model can be illustrated as a recursive optimization procedure that consists of three major modules (see Figure 1):

1. *Data processing.* The signal-timing data obtained from the previous control cycle, including gap-out/max-out information, phase splits, and parameter settings (e.g., minimum green, maximum green, unit extension), are used to produce a new dataset that represents the current traffic condition associated with each actuated phase: vehicle arrival flow, vehicle departure (i.e., the number of vehicles that have entered the intersection) and vehicle spillover (i.e., the number of vehicles that have not entered the intersection).
2. *Flow prediction.* A traffic flow prediction algorithm that is an extension of the previous work (Liu, Sun, and Recker, 2005) applies here to (a) estimate the approaching flow toward the downstream intersection on the basis of the vehicle departures from upstream signal phases and (b) estimate the turning fractions associated with each downstream signal phase based on the vehicle arrival flow in previous cycles at the downstream intersection. Then, the future arrival flow for each signal phase at the downstream intersection is determined by multiplying the approaching flow and the corresponding turning fraction.
3. *Parameter optimization*. In the approach taken here, we restrict our attention to only those control parameters that are commonly found in modern actuated controllers: maximum

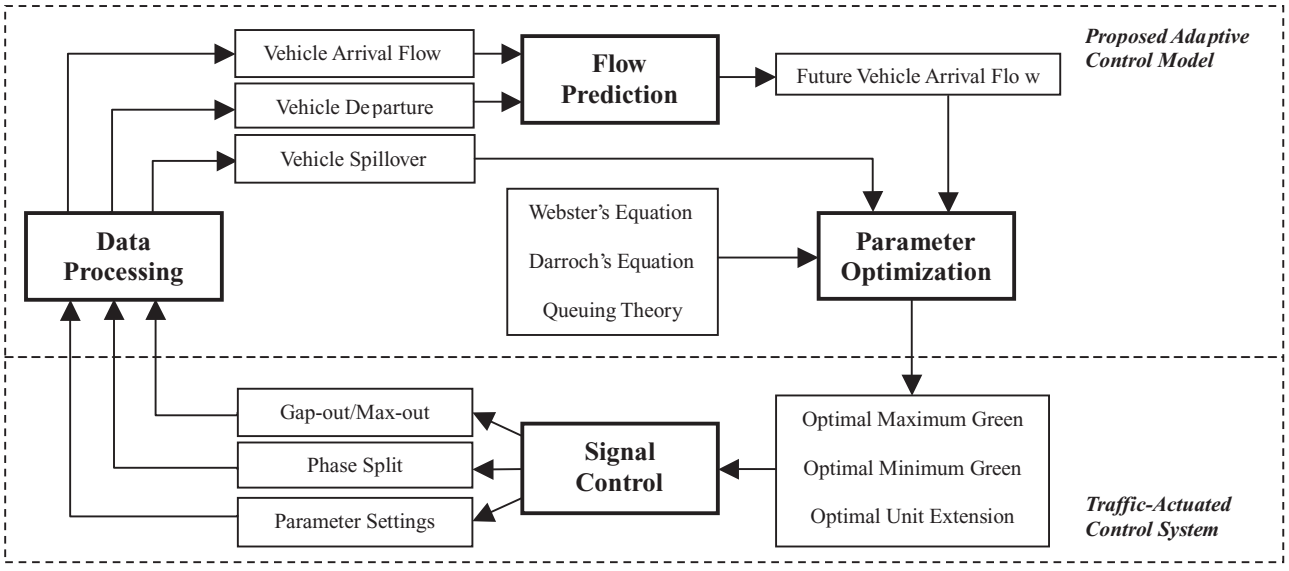

Figure 1 Recursive optimization procedure.

green, minimum green, and unit extension (i.e., passage time, gap, vehicle interval). Such other control parameters as phase sequence and yellow and red clearance are predefined regarding safety and geometric considerations and are not adjusted.

Maximum green time is optimized according to the effective green factor determined with the Webster's equation (Webster, 1958). This equation is expressed in terms of the vehicle spillover and future arrival flow. On the basis of the critical path-seeking logic, the maximum green is determined for all actuated phases.

A nonlinear optimization problem is formulated on the basis of the approach taken by McNeil (1968). The objective is to minimize total intersection control delay per cycle, and the solution is a set of optimal phase splits (i.e., phase durations) for all actuated phases. The delay expression is given by Darroch (1964), which is a generalization of the well-known Webster formulation and is also expressed in terms of the vehicle spillover and future arrival flow. The optimized phase splits will be used to determine optimal minimum green and unit extension.

Minimum green time is optimized according to the queue service time. Similar to the added initial in volume-density control, the minimum green computed here is a variant and has a maximum limit. On the basis of the queuing theory (Kleinrock, 1975), the variant minimum green is expressed in terms of the vehicle spillover, future arrival flow, and optimized phase split.

The optimal unit extension is expected to be a gap time that invokes gap-out control at the end of the optimized phase split. Also, it is also expressed in terms of the vehicle spillover, future arrival flow, and optimized phase split.

These optimized timing parameters are used for the upcoming control cycle as well as to provide signal-timing data for further optimizations. The following is a list of assumptions and explications:

1. The proposed model is formulated on the basis of the basic operation logic of full-actuated controllers. Other actuated control modes, such as semi-actuated and volume density, are not considered.
2. Signal timing relies on the basic gap-seeking logic of actuated control. Special operation functions, such as double cycle, are not considered.
3. Effective green time is assumed to be equal to the actual displayed green interval, and the total lost time for each signal phase is assumed to be constant.
4. The vehicle arrival pattern is assumed to be a Poisson process (strictly speaking, this assumption limits the application of the model to noncongested periods of operation).
5. Vehicle arrival flow rate is assumed to be strictly less than the saturation flow rate, and the saturation flow rate for each signal phase is assumed to be constant.
6. Right-turn movements are assumed to be serviced on exclusive right-turn lanes and have negligible effect on the signal operation. U-turn movements and midblock situations are not considered.

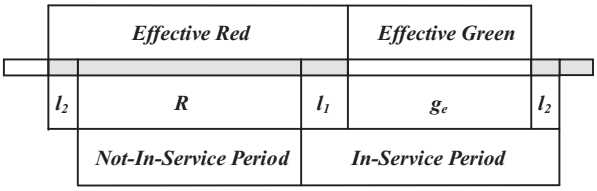

Figure 2 Phase state.

7. In the proposed control model, all timing-related variables take expected or average values.

The notations used in the model formulation appear in the Appendix.

Processing Signal-timing Data

In general, a signal-control phase changes its state alternatively between *in service* and *not in service* within the whole timing period. Each *in-service* period is defined as the phase split (including lost time), and each *not-in-service* period is defined as the red duration, which is actually the in-service period for conflicting phases. From another viewpoint, the phase state changes alternatively between *effective green* and *effective red*. *Effective green* refers to the period from the end of startup lost time to the beginning of clearance lost time within the same phase, and *effective red* refers to the period preceding effective green, which consists of total lost time and red duration. The relations between these timing periods are shown in Figure 2 and can be expressed as follows:

$$G = l_1 + g_e + l_2 = g_e + L \tag{1}$$

$$r_e = l_2 + R + l_1 = R + L \tag{2}$$

$$G + R = g_e + r_e \tag{3}$$

According to the *Highway Capacity Manual* (TRB, 2000), effective green time can be further broken into queue service time and green extension period (see Figure 3). During queue service time, vehicles discharge at saturation flow rate until the

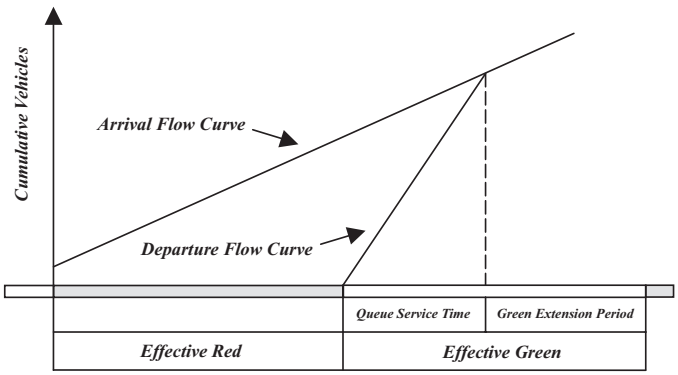

Figure 3 Queuing accumulation diagram.

queue dissipates. The total number of these vehicles is equal to the sum of initial queue, if any, plus those vehicles that arrive during effective red and queue service time:

$$S \times G_q = Q + \lambda \times (R + L) + \lambda \times G_q \tag{4}$$

Then, the queue service time can be expressed as follows:

$$G_q = [Q + \lambda \times (R + L)] / (S - \lambda) \tag{5}$$

The vehicle departure number in queue service time is determined by the following:

$$N(G_q) = S \times [Q + \lambda \times (R + L)] / (S - \lambda) \tag{6}$$

During green extension period, arriving vehicles travel through the intersection freely until the current phase terminates by gap-out control—the green interval terminates when no vehicles actuate the extension detector within a unit extension period; that is, when the vehicle headway (in time) larger than unit extension occurs. According to Poisson process, vehicle headways have a negative exponential distribution and the number (n) of headways until the first one invokes gap-out (i.e., larger than β) has a geometric distribution:

$$P_{robability}(\text{number of headways until the first one larger than } \beta \text{ occurs}) = [1 - \exp(-\lambda\beta)]^{n-1} \exp(-\lambda\beta)$$
$$M_{ean}(\text{number of headways until the first one larger than } \beta \text{ occurs}) = \exp(\lambda\beta).$$

During the $e^{\lambda\beta}$ vehicle headways, total of $(e^{\lambda\beta} - -1)$ vehicles are serviced. Thus, the vehicle departure number in green extension period is determined by the following:

$$N(G_e) = \exp(\lambda\beta) - 1 \tag{7}$$

And, the green extension period can be expressed by the following:

$$G_e = [\exp(\lambda\beta) - 1] / \lambda \tag{8}$$

It should be noted here that the green-time estimation model mentioned in the *Highway Capacity Manual* is formulated on the basis of two indefensible assumptions: (a) the extension detector is placed at the stop line and thus the green extension period starts timing when queue service time expires and (b) the signal phase definitely terminates by gap-out control. In real field situations, however, the extension detector, especially the one for through movement phases, is set back a certain distance (e.g., 200 feet) from the stop line, and max-out control materializes frequently when the traffic demand increases. In addition, according to the timing logic of actuated controllers, the green extension period starts timing exactly when minimum green expires, so it is possible that the phase terminates by gap-out control while the queue has not dissipated. To avoid these shortcomings, we herein take into account both the gap-out/max-out information and the signal-timing data that includes minimum green, maximum green, and unit extension to determine the effective green time as well as the number of vehicle departure and spillover for the expired actuated phases. For the sake of simplicity, it is assumed that when the minimum green time expires, the vehicle queue length has been decreased to be shorter than the distance from the trailing edge of the extension detector to the stop line.

Gap-out situation

When a signal phase terminates by gap-out control, the green extension period; that is, the period from the end of minimum green to the end of green interval, can still be expressed by Equation (8) unless the arrival pattern changes. Thus, the effective green is equal to minimum green plus green extension period, i.e.,

$$g_e = G_{\min} + [\exp(\lambda\beta) - 1] / \lambda \tag{9}$$

Then, the phase split is expressed by the following:

$$G = G_{\min} + [\exp(\lambda\beta) - 1] / \lambda + L \tag{10}$$

In Equation (10), all variables except λ are known signal-timing parameters obtained from the expired phase, and thus the vehicle arrival flow rate λ can be determined by solving the nonlinear inverse function $F^{-1}(\lambda)$, i.e.,

$$\lambda = F^{-1}(\lambda); \tag{11}$$

where

$$F(\lambda) = G_{\min} + [\exp(\lambda\beta) - 1] / \lambda + L - G = 0$$

To determine the vehicle departure and spillover, three cases that describe different gap-out situations need to be considered (see Figure 4).

1.

$$\begin{aligned} &G_q \le G_{\min} \\ &\text{i.e;} [Q + \lambda \times (R + L)] / (S - \lambda) \le G_{\min} \\ &\text{or,} \lambda \le (S \times G_{\min} - Q) / (R + L + G_{\min}) \end{aligned} \tag{12}$$

2.

$$\begin{aligned} &G_{\min} < G_q \le g_e \\ &\text{i.e.,} G_{\min} < [Q + \lambda \times (R + L)] / (S - \lambda) \le G - L \\ &\text{or,} (S \times G_{\min} - Q) / (R + L + G_{\min}) < \lambda \\ &\quad \le [S \times (G - L) - Q] / (R + G) \end{aligned} \tag{13}$$

3.

$$\begin{aligned} &g_e < G_q \\ &\text{i.e.,} G - L < [Q + \lambda \times (R + L)] / (S - \lambda) \\ &\text{or,} \lambda > [S \times (G - L) - Q] / (R + G) \end{aligned} \tag{14}$$

As can be seen, three consecutive, nonoverlapped numerical intervals regarding to the value of λ are illustrated by Inequalities (12), (13), and (14), which are also expressed in terms of known timing parameters. On the basis of the λ determined by Equation (11), only one inequality (i.e., only one case) is *true*. Therefore,

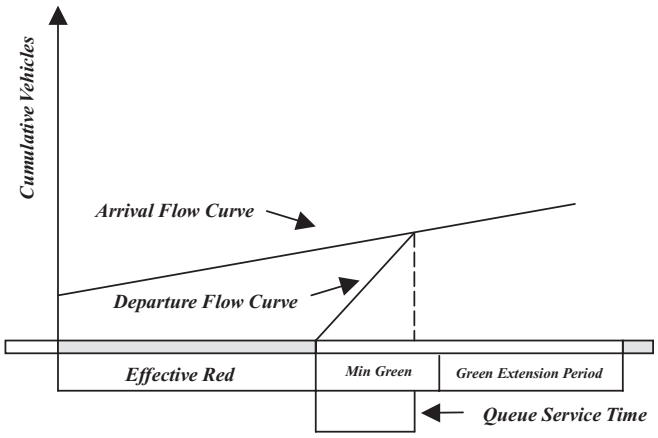

(a) Case 1

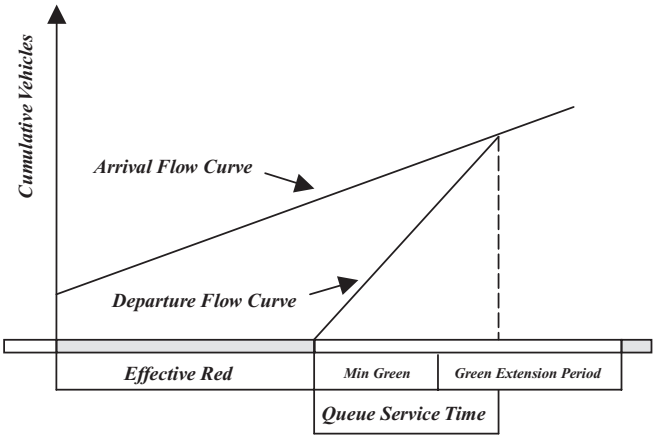

(b) Case 2

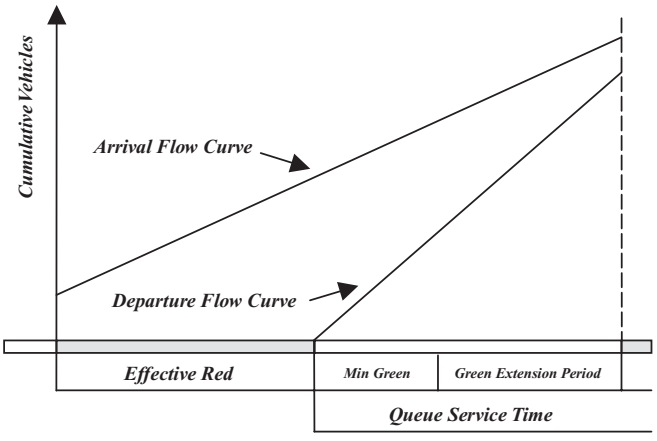

(c) Case 3

Figure 4 Gap-out situations. (a) Case 1. (b) Case 2. (c) Case 3.

the vehicle departure and spillover can be determined by the following equations that correspond to the true case.

Case 1 or 2:

$$N(G) = N\left(G_q\right) + \left(G - L - G_q\right) \times \lambda \tag{15}$$

$$Q^{spill} = 0 \tag{16}$$

Case 3:

$$N(G) = (G - L) \times S \tag{17}$$

$$Q^{spill} = Q + \lambda \times (G + R) - N(G) \tag{18}$$

Max-out situation

When a signal phase terminates by max-out control, the green extension period—the period from the end of minimum green to the end of green interval—cannot be expressed by Equation (8), and the effective green is equal to maximum green; that is, the following:

$$g_e = G_{\max} \tag{19}$$

Therefore, the phase split is expressed by the following:

$$G = G_{\max} + L \tag{20}$$

Unlike Equation (10), although the variables in Equation (20) are known signal-timing parameters, the vehicle arrival flow rate λ cannot be determined. Considering the fact that arriving vehicles keep actuating the extension detector until maximum green limit is reached, it is safe to presume that the vehicle number arriving during the green extension period is greater than the least vehicle number that invokes max-out control; that is, the following:

$$\lambda \times G_e \geq G_e/\beta \text{ or } \lambda \geq 1/\beta \tag{21}$$

Specifically, we assume here that λ is approximately equal to the mean of $1/\beta$ and S; that is, the following:

$$\lambda = \left(1/\beta + S\right)/2 \tag{22}$$

To determine the vehicle departure and spillover, three cases that describe different max-out situations need to be considered (Figure 5).

1.

$$\begin{aligned} &G_q \leq G_{\min} \\ &\text{i.e., } [Q + \lambda \times (R + L)]/(S - \lambda) \leq G_{\min} \\ &\text{or, } \lambda \leq (S \times G_{\min} - Q)/(R + L + G_{\min}) \end{aligned} \tag{23}$$

2.

$$\begin{aligned} &G_{\min} < G_q \leq g_e \\ &\text{i.e., } G_{\min} < [Q + \lambda \times (R + L)]/(S - \lambda) \leq G_{\max} \\ &\text{or, } (S \times G_{\min} - Q)/(R + L + G_{\min}) < \lambda \\ &\quad \leq [S \times G_{\max} - Q]/(R + L + G_{\max}) \end{aligned} \tag{24}$$

3.

$$\begin{aligned} &g_e < G_q \\ &\text{i.e., } G_{\max} < [Q + \lambda \times (R + L)]/(S - \lambda) \\ &\text{or, } \lambda > [S \times G_{\max} - Q]/(R + L + G_{\max}) \end{aligned} \tag{25}$$

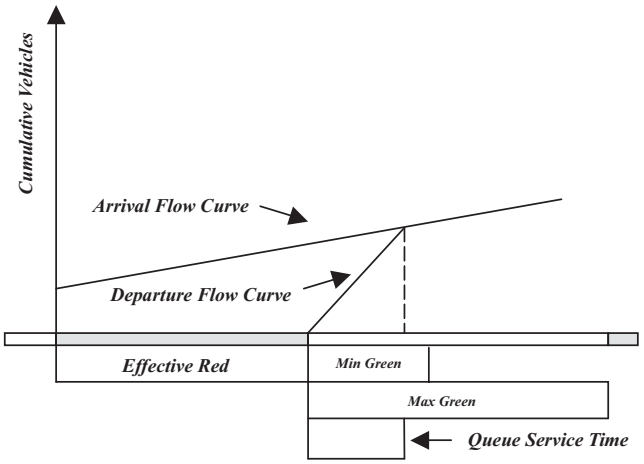

(a) Case 1

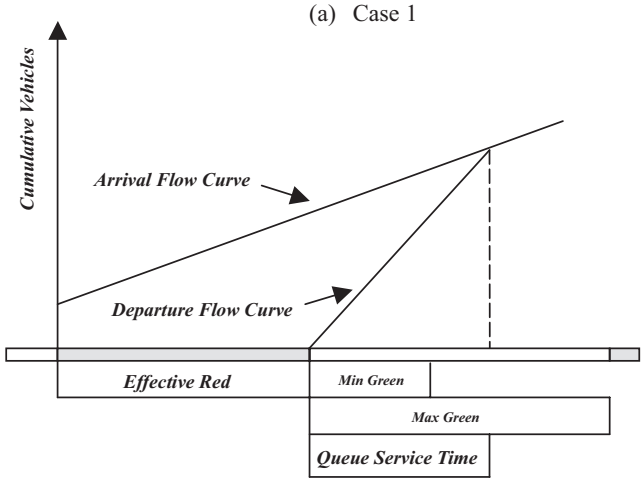

(b) Case 2

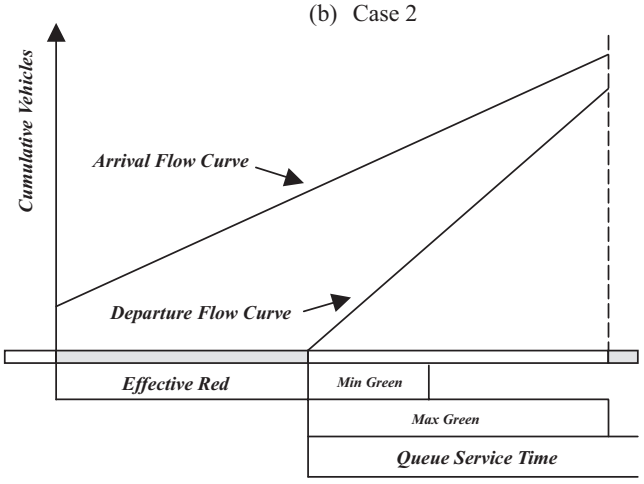

(c) Case 3

Figure 5 Max-out situations. (a) Case 1. (b) Case 2. (c) Case 3.

Similarly, on the basis of the λ determined by Equation (22), only one of Inequalities (23), (24), and (25) is *true*. Therefore, the vehicle departure and spillover can be determined by the following equations that correspond to the true case.

Case 1 or 2:

$$N(G) = N(G_q) + (G_{\max} - G_q) \times \lambda \tag{26}$$

$$Q^{spill} = 0 \tag{27}$$

Case 3:

$$N(G) = G_{\max} \times S \tag{28}$$

$$Q^{spill} = Q + \lambda \times (G_{\max} + L + R) - N(G) \tag{29}$$

For the sake of generality, the following prediction and optimization algorithms are formulated on the basis of the timing process of the standard National Electrical Manufacturers Association (NEMA) eight-phase full-actuated dual-ring controller. Phases 1 to 4 are assigned in Ring A, and Phases 5 to 8 are assigned in Ring B, with leading left-turn phases on either side of the barrier. Superscript j denotes the expired or current control cycle, $j+1$ denotes the upcoming or objective control cycle, and so forth. Subscripts i, n, and r, if not specifically designated, denote each signal phase.

Estimating arrival flow

In a signalized network, the approaching flow toward the downstream intersection is contributed by the vehicle departures from corresponding signal phases of upstream intersection. Referring to the example shown in Figure 6, two signalized intersections are connected by a single link, and both signals operate under dual-ring actuated control. As can be seen, the approaching flow is actually the combined departure flow generated from the left-turn phase (Phase 3) and the through phase (Phase 6) of intersection k, and it consists of the inflows for the left-turn phase (Phase 1) and the through phase (Phase 6) of downstream intersection m. Because right-turn movements are assumed to be serviced on exclusive right-turn lanes and have negligible effect on signal timing, the departure and arrival flows corresponding to these movements are not considered here.

On the basis of the vehicle departure number obtained from the previous section, the departure flow of a signal phase at the

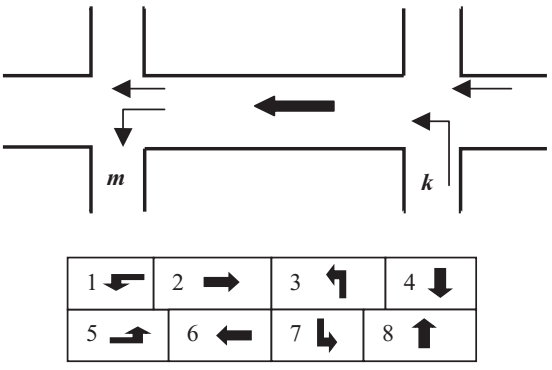

Figure 6 Approaching flow.

upstream intersection is determined by the following:

$$q_i^j = N\left(G_i^j\right)\Big/C^j \tag{30}$$

where

$$C^j = G_1^j + G_2^j + G_3^j + G_4^j = G_5^j + G_6^j + G_7^j + G_8^j$$

Therefore, in this example, the approaching flow is determined by the following:

$$q_{3k}^j + q_{6k}^j = \left[N\left(G_{3k}^j\right) + N\left(G_{6k}^j\right)\right]\Big/C_k^j \tag{31}$$

where

$k =$ index of the upstream intersection or signal

Because the generation of approaching flow (at the upstream intersection) occurs earlier than the reception (at the downstream intersection), the phase-departure flow from upstream signal in the previous cycles and ongoing cycle can be considered to be the future approaching flow toward the downstream signal.

Alternatively, the turning fraction associated with each signal phase at the downstream intersection is determined on the basis of the vehicle arrival flow obtained from the previous section. In this example, the turning fraction associated with each phase of the downstream signal is determined by the following:

$$\begin{aligned} TF_{1m}^j &= \lambda_{1m}^j\Big/\left(\lambda_{1m}^j + \lambda_{6m}^j\right) \\ TF_{6m}^j &= \lambda_{6m}^j\Big/\left(\lambda_{1m}^j + \lambda_{6m}^j\right) \end{aligned} \tag{32}$$

where

$m =$ index of the downstream intersection or signal

To estimate the future turning fraction in upcoming cycles, we use the exponential smoothing model here:
Define

$TF_i^j =$ the true value of turning fraction as determined by Eq. (32)

$TF_i^{(est)\,j} =$ the estimated value of turning fraction

$a_i^j =$ the smoothing factor

Then,

$$\begin{aligned} &TF_i^{(est)\,j+1} = a_i^j \times TF_i^j + \left(1 - a_i^j\right) \times TF_i^{(est)\,j} \text{or,} \\ &TF_{i^{j+1}}^{(est)} = TF_{i^j}^{(est)} + a_i^j \times \left(TF_i^j - TF_{i^j}^{(est)}\right), 0 < a_i^j \le 1 \end{aligned} \tag{33}$$

Therefore, in this example, the future arrival flow rate associated with each signal phase at the downstream intersection is determined by the following:

$$\begin{aligned} \lambda_{1m}^{j+1} &= TF_{1m^{j+1}}^{(est)} \times \left(q_{3k}^j + q_{6k}^j\right) \\ \lambda_{6m}^{j+1} &= TF_{6m^{j+1}}^{(est)} \times \left(q_{3k}^j + q_{6k}^j\right) \end{aligned} \tag{34}$$

It should be noted here that the value of smoothing factor a can be any positive decimal (≤ 1), and is usually set small for slowly evolving conditions and large for significant transients. The properties of exponential smoothing model can be found elsewhere (Chou, 1970). Herein, the initial value of a is arbitrarily determined (e.g., 0.3), and, if significant errors exist, it will be updated every signal control cycle by substituting the true value into Equation (33); that is, the following:

$$a_i^{j+1} = \left(TF_i^{j+1} - TF_{i^j}^{(est)}\right)\Big/\left(TF_i^j - TF_{i^j}^{(est)}\right) \tag{35}$$

Determining optimal maximum green

In determining maximum green time, Webster's (1958) equation is used to express the effective green factor:

$$D_i^{j+1} = \left[\lambda_i^{j+1} + Q_i^{j+1} \times \left(3600\big/C_{\max}\right)\right]\Big/S_i \tag{36}$$

In Equation (36), term λ_i^{j+1} is the future vehicle arrival flow rate as determined by Equation (34). Term Q_i^{j+1} is the initial queue in cycle j+1 and equals to the vehicle spillover in cycle j; that is, the following:

$$Q_i^{j+1} = \left(Q^{spill}\right)_i^j \tag{37}$$

Maximum green-time setting is actually to distribute maximum allowable effective green among all actuated phases and usually consists of two computation steps: determination of the critical path and allocation of the effective green time. The critical path is composed of the critical path for each side of the dual-ring structure, which is determined by the following:
Left Critical Path

$$D_m^{j+1} + D_n^{j+1} = \max\left[D_1^{j+1} + D_2^{j+1}, D_5^{j+1} + D_6^{j+1}\right] \tag{38}$$

Right Critical Path

$$D_r^{j+1} + D_k^{j+1} = \max\left[D_3^{j+1} + D_4^{j+1}, D_7^{j+1} + D_8^{j+1}\right] \tag{39}$$

where $m, n = 1, 2$ or $5, 6$ and $r, k = 3, 4$ or $7, 8$

Therefore, the effective green allocated to each side of the dual-ring structure is determined by the following:

$$\begin{aligned} g_{e(left)}^{j+1} &= g_{e(cycle)} \times \left(D_m^{j+1} + D_n^{j+1}\right) \\ &\quad\Big/\left[\left(D_m^{j+1} + D_n^{j+1}\right) + \left(D_r^{j+1} + D_k^{j+1}\right)\right] \\ g_{e(right)}^{j+1} &= g_{e(cycle)} \times \left(D_r^{j+1} + D_k^{j+1}\right) \\ &\quad\Big/\left[\left(D_m^{j+1} + D_n^{j+1}\right) + \left(D_r^{j+1} + D_k^{j+1}\right)\right] \end{aligned} \tag{40}$$

where $g_{e(cycle)} = C_{\max} - (L_m + L_n + L_r + L_k)$

Then, the maximum effective green (or maximum green) allocated to each phase on the critical path is determined by the following:

$$G_{\max m}^{j+1} = g_{e(left)}^{j+1} \times D_m^{j+1}\Big/\left(D_m^{j+1} + D_n^{j+1}\right) \tag{41}$$

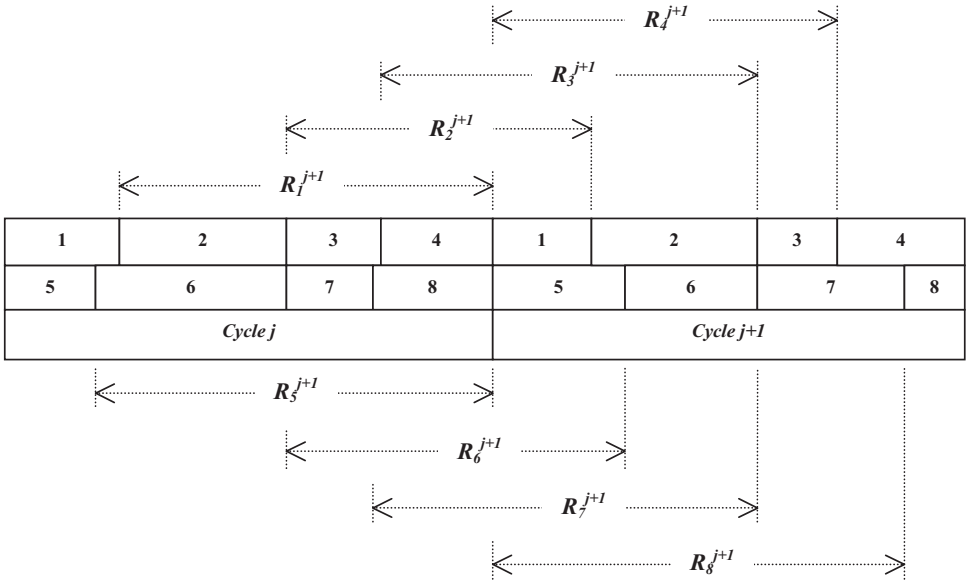

Figure 7 Expression of red duration.

$$G_{\max n}^{j+1} = g_{e(left)}^{j+1} \times D_n^{j+1} \Big/ \left(D_m^{j+1} + D_n^{j+1}\right) \tag{42}$$

$$G_{\max r}^{j+1} = g_{e(right)}^{j+1} \times D_r^{j+1} \Big/ \left(D_r^{j+1} + D_k^{j+1}\right) \tag{43}$$

$$G_{\max k}^{j+1} = g_{e(right)}^{j+1} \times D_k^{j+1} \Big/ \left(D_r^{j+1} + D_k^{j+1}\right) \tag{44}$$

For the phases that are not on the critical path, the maximum green can be determined using the same philosophy as shown from Equations (41) to (44).

Determining optimal phase split

A nonlinear optimization problem is formulated to determine optimal phase splits, with the objective to be minimizing total intersection control delay during the upcoming cycle. The delay expression is given by Darroch (1964), which is a generalization of the well-known Webster (1958) formulation:

$$W_i^{j+1} = S_i \times \lambda_i^{j+1} \times \left\{ \left(R_i^{j+1}\right)^2 + R_i^{j+1} \left[2Q_i^{j+1} \Big/ \lambda_i^{j+1} + 1 \Big/ S_i + 1 \Big/ \left(S_i - \lambda_i^{j+1}\right) \right] \right\} \Big/ \left[2\left(S_i - \lambda_i^{j+1}\right) \right] \tag{45}$$

Also, the optimization problem is expressed by the following:

$$Min \sum_i W_i^{j+1}, \text{ where } i = 1, 2, ..., 8 \tag{46}$$

In Equation (45), the term R_i^{j+1} is the red duration, determined by summing up the splits of these conflicting phases in the same ring preceding the study phase on the basis of the circular dependency relation in dual-ring structure (see Figure 7); that is, the following:

$$\begin{aligned}
R_1^{j+1} &= G_2^j + G_3^j + G_4^j \\
R_2^{j+1} &= G_1^{j+1} + G_3^j + G_4^j \\
R_3^{j+1} &= G_1^{j+1} + G_2^{j+1} + G_4^j \\
R_4^{j+1} &= G_1^{j+1} + G_2^{j+1} + G_3^{j+1} \\
R_5^{j+1} &= G_6^j + G_7^j + G_8^j \\
R_6^{j+1} &= G_5^{j+1} + G_7^j + G_8^j \\
R_7^{j+1} &= G_5^{j+1} + G_6^{j+1} + G_8^j \\
R_8^{j+1} &= G_5^{j+1} + G_6^{j+1} + G_7^{j+1}
\end{aligned} \tag{47}$$

It can be realized that Equation (47) does not contain the terms G_4^{j+1} and G_8^{j+1}, and thus Equation (46) cannot be expressed in terms of all objective phase splits. To solve this problem, a rolling horizon scheme is used in the present article.

Revise Equation (47) to the following:

$$\begin{aligned}
R_1^{j+2} &= G_2^{j+1} + G_3^{j+1} + G_4^{j+1} \\
R_2^{j+1} &= G_1^{j+1} + G_3^j + G_4^j \\
R_3^{j+1} &= G_1^{j+1} + G_2^{j+1} + G_4^j \\
R_4^{j+1} &= G_1^{j+1} + G_2^{j+1} + G_3^{j+1} \\
R_5^{j+2} &= G_6^{j+1} + G_7^{j+1} + G_8^{j+1} \\
R_6^{j+1} &= G_5^{j+1} + G_7^j + G_8^j \\
R_7^{j+1} &= G_5^{j+1} + G_6^{j+1} + G_8^j \\
R_8^{j+1} &= G_5^{j+1} + G_6^{j+1} + G_7^{j+1}
\end{aligned} \tag{48}$$

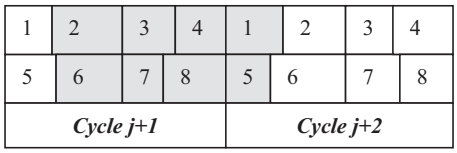

Figure 8 Actual objective cycle.

Accordingly, the optimization problem becomes the following:

$$Min\left(\sum_i W_i^{j+1} + \sum_r W_r^{j+2}\right),$$

$$\text{where } i = 2, 3, 4, 6, 7, 8 \text{ and } r = 1, 5 \tag{49}$$

As can be seen, the problem objective becomes to minimize the intersection control delay in a different period other than the cycle composed of target phases (see Figure 8). Again, on the basis of the circular dependency relation, Phase 1 in Cycle $j+2$ follows Phase 4 in Cycle $j+1$, and Phase 5 in Cycle $j+2$ follows Phase 8 in Cycle $j+1$. Therefore, in this sense, the objective function still minimizes the control delay per cycle (highlighted in gray) except that this cycle may not match in both rings. Nevertheless, the objective cycle in the next optimization procedure starts from Phase 2 in Ring A and Phase 6 in Ring B of Cycle $j+2$.

Two constraints are considered in formulating the optimization problem:

1. *Barrier condition.* According to the concept of dual-ring signal control, the timing period in Ring A should be equal to the timing period in Ring B on either side of the barrier:

$$\begin{aligned} G_1^{j+1} + G_2^{j+1} &= G_5^{j+1} + G_6^{j+1} \\ G_3^{j+1} + G_4^{j+1} &= G_7^{j+1} + G_8^{j+1} \end{aligned} \tag{50}$$

1. *Equilibrium condition*. The phase green is expected to be large enough to service all the vehicles that arrive during the effective red and effective green (plus initial queue) to avoid oversaturation delay; that is, to terminate the phase by gap-out control and invokes no vehicle spillover—referring to gap-out Case 1 and 2, Figures 4(a) and 4(b):

$$G_i^{j+1} < G_{\max i}^{j+1} + L_i \tag{51}$$

and

$$G_{qi}^{j+1} \le G_i^{j+1} - L_i \tag{52}$$

where

$$G_{qi}^{j+1} = \left[Q_i^{j+1} + \lambda_i^{j+1} \times \left(R_i^{j+1} + L_i\right)\right] \Big/ \left(S_i - \lambda_i^{j+1}\right)$$

Then, the complete optimization problem is expressed by the following:

$$Min\left(\sum_i W_i^{j+1} + \sum_r W_r^{j+2}\right),$$
$$\text{where } i = 2, 3, 4, 6, 7, 8 \text{ and } r = 1, 5$$

subject to

$$\begin{aligned} G_1^{j+1} + G_2^{j+1} &= G_5^{j+1} + G_6^{j+1} \\ G_3^{j+1} + G_4^{j+1} &= G_7^{j+1} + G_8^{j+1} \\ G_{qi}^{j+1} + L_i \le G_i^{j+1} &< G_{\max i}^{j+1} + L_i \end{aligned}$$

Determining optimal minimum green

Traditionally, minimum green is set equal to an initial green period that allows all vehicles potentially stored between the setback detector (e.g., extension detector) and the stop line to enter the intersection (particularly for through movement phases). This setting assumes that the entire distance between the detector and the stop line is occupied by stored vehicles, an assumption that is violated under light traffic conditions. Referring to Figure 4(a), for example, the required queue service time is less than the minimum green; that is, queuing vehicles (stored vehicles plus those vehicles joining the queue) will enter the intersection before minimum green expires, and thus the minimum green will not be fully used and the signal phase may terminate by gap-out control later. This weakness is mitigated in volume-density control, in which minimum green (or, added initial) is calculated on the basis of the counted number of stored vehicles, and this computed initial green cannot exceed a preset maximum limit (i.e., maximum initial). A similar method is taken here to determine minimum green: set minimum green equal to queue service time if queue service time is less than the predetermined (i.e., traditional) minimum green, G_{mini}^0, otherwise, set it equal to the predetermined minimum green; that is, the following:

$$\begin{aligned} G_{\min i}^{j+1} &= \begin{cases} G_{qi}^{j+1} \text{ if } G_{qi}^{j+1} \le G_{\min i}^0 \\ G_{\min i}^0 \text{ if } G_{qi}^{j+1} > G_{\min i}^0 \end{cases} \text{ or,} \\ G_{\min i}^{j+1} &= \min\left[G_{qi}^{j+1}, G_{\min i}^0\right] \end{aligned} \tag{53}$$

Determining optimal unit extension

Recall that the optimized phase is expected to be terminated by gap-out control; therefore, the phase split can be expressed by Equation (10):

$$G_i^{j+1} = G_{\min i}^{j+1} + \left[\exp\left(\lambda_i^{j+1}\beta_i^{j+1}\right) - 1\right] \Big/ \lambda_i^{j+1} + L_i \tag{54}$$

Then,

$$\beta_i^{j+1} = \ln\left[1 + \lambda_i^{j+1} \times \left(G_i^{j+1} - L_i - G_{\min i}^{j+1}\right)\right] \Big/ \lambda_i^{j+1} \tag{55}$$

It should be noted that the natural logarithm in Equation (55) requires $[1 + \lambda \times (G - L - G_{min})]$ be greater than 0. According to Inequality (52):

$$G_{qi}^{j+1} \le G_i^{j+1} - L_i$$

we have the following:

$$G_{qi}^{j+1} - G_{\min i}^{j+1} \le G_i^{j+1} - L_i - G_{\min i}^{j+1} \tag{56}$$

According to Equation (53), we have the following:

$$\begin{aligned} &G_{qi}^{j+1} - G_{qi}^{j+1} \le G_i^{j+1} - L_i - G_{\min i}^{j+1} \text{ if } G_{qi}^{j+1} \le G_{\min i}^{0} \\ &G_{qi}^{j+1} - G_{\min i}^{0} \le G_i^{j+1} - L_i - G_{\min i}^{j+1} \text{ if } G_{qi}^{j+1} > G_{\min i}^{0} \\ &0 \le G_i^{j+1} - L_i - G_{\min i}^{j+1} \text{ if } G_{qi}^{j+1} \le G_{\min i}^{0} \\ &0 < G_i^{j+1} - L_i - G_{\min i}^{j+1} \text{ if } G_{qi}^{j+1} > G_{\min i}^{0} \end{aligned} \quad \text{or,} \tag{57}$$

Then,

$$\begin{aligned} &1 \le 1 + \lambda_i^{j+1} \times \left(G_i^{j+1} - L_i - G_{\min i}^{j+1} \right) \text{ if } G_{qi}^{j+1} \le G_{\min i}^{0} \\ &1 < 1 + \lambda_i^{j+1} \times \left(G_i^{j+1} - L_i - G_{\min i}^{j+1} \right) \text{ if } G_{qi}^{j+1} > G_{\min i}^{0} \end{aligned} \tag{58}$$

The requirement of natural logarithm is satisfied. Also, substituting Inequality (58) into Equation (55) yields the following:

$$\begin{aligned} &\beta_i^{j+1} \ge 0 \text{ if } G_{qi}^{j+1} \le G_{\min i}^{0} \\ &\beta_i^{j+1} > 0 \text{ if } G_{qi}^{j+1} > G_{\min i}^{0} \end{aligned} \tag{59}$$

TESTING AND EVALUATION

The proposed adaptive signal control model is tested and evaluated using a scalable, high-performance microscopic simulation package, PARAMICS (Cameron and Duncan, 1996). PARAMICS has been widely used in the testing and evaluation of various intelligent transportation system strategies because of its powerful application programming interfaces, through which users can access the core functions to extend and customize many features of the underlying simulation model, without having to deal with the proprietary source codes. The proposed control model is developed as a PARAMICS plug-in through API programming.

The study network is as shown in Figure 9, which is called *Irvine Triangle*, located in southern California. A previous study calibrated this network for the morning peak period from 6 a.m. to 10 a.m. (Chu, Liu, and Recker, 2004). This network includes a 6-mile section of freeway I-405, a 3-mile section of freeway I-5, a 3-mile section of freeway SR-133 and several adjacent surface streets, including two streets parallel to I-405 (i.e., Alton Parkway and Barranca Parkway), one street parallel to I-5 (i.e., Irvine Center Drive), and three crossing streets to I-405 (i.e. Culver Drive, Jeffery Road, and Sand Canyon Avenue). A total of 38 signals under free-mode actuated control are included in the original network.

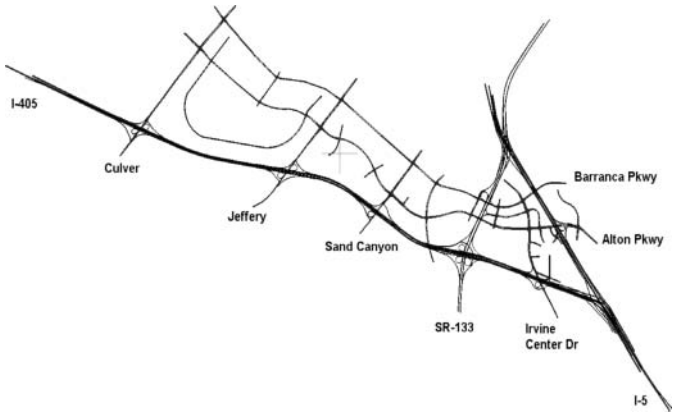

Figure 9 Test network.

The maximum allowable cycle length, C_{max}, is set equal to 100 s for each signal. The total lost time, L, is assumed 4 s for each actuated phase. The saturation flow rate, S, is set equal to 1,900 vehicles per hour per lane for each through movement phase, and 1,800 vehicles per hour per lane for each left-turn movement phase. To make the proposed control algorithm more practical, the optimized control parameters that take extremely small values are further adjusted on the basis of the following rules:

(1) If the minimum green time is extremely short (e.g., <4 s), it is set to be 4 s.
(2) If the maximum green time is shorter than the minimum green time, it is set equal to the minimum green.
(3) If the unit extension is not greater than $1/S$, which may cause premature gap-out right after the minimum green, it is set equal to $1/S + 0.1$ s.

In this study, three traffic demand scenarios are set up for the model evaluation:

1. *Existing-demand scenario.* This scenario corresponds to the traffic condition for the morning peak period and demands are obtained directly from the calibrated simulation model.
2. *Medium-demand scenario*. This scenario's demands are equivalent to 75% of the existing demand scenario.
3. *Low-demand scenario.* This scenario's demands are equivalent to 50% of the existing demand scenario.

Simulations are performed for a period of 4 hr and 15 min for each scenario under baseline control and adaptive control respectively. The baseline control corresponds to the free-mode actuated control strategy applied in the existing network. The first 15 min are considered to be the warm-up period for vehicles to fill in the network to represent the typical traffic condition at the start time of simulation (i.e., 6 a.m.) when the traffic condition is free-flow—it takes less than 10 min for a vehicle to finish the longest trip in the network in the real world.

Table 1a Simulation results of the network (Scenario 1).

Variable	Average Travel Time (seconds)	Average Vehicle Speed (miles per hour)	Vehicle Mileage Traveled (miles)	Vehicle Hours Traveled (hours)
Baseline control				
M	344.3	43.9	760920.0	17367.6
SD	3.5	0.5	2589.8	159.3
Number of required runs	0.9	0.1	1.1	1.0
Adaptive control				
M	331.0	45.9	762491.2	16725.5
SD	5.1	1.0	5781.8	244.0
Number of required runs	2.2	0.6	4.8	2.5

Table 1b Simulation results of the network (Scenario 2).

Variable	Average Travel Time (seconds)	Average Vehicle Speed (miles per hour)	Vehicle Mileage Traveled (miles)	Vehicle Hours Traveled (hours)
Baseline control				
M	257.0	59.1	575585.6	9788.2
SD	1.4	0.2	1602.1	32.1
Number of required runs	0.1	0.1	0.1	0.3
Adaptive control				
M	255.2	59.5	576046.1	9671.8
SD	0.6	0.2	1895.5	36.1
Number of required runs	0.1	0.1	0.1	0.3

Table 1c Simulation results of the network (Scenario 3).

Variable	Average Travel Time (seconds)	Average Vehicle Speed (miles per hour)	Vehicle Mileage Traveled (miles)	Vehicle Hours Traveled (hours)
Baseline control				
M	249.5	60.9	382327.4	6284.3
SD	0.4	0.1	1172.8	22.5
Number of required runs	0.1	0.1	0.0	0.0
Adaptive control				
M	248.4	61.1	382649.9	6263.4
SD	0.3	0.1	742.0	20.1
Number of required runs	0.1	0.1	0.0	0.0

Two groups of performance measures are used for the model evaluation. For the whole network, the following are used: average travel time, average vehicle speed, vehicle mileage traveled, and vehicle hours traveled. For local intersections, the following are used: vehicle spillover, maximum queue length, and vehicle travel delay.

It should be noted here that PARAMICS is a stochastic simulation model that introduces random effects in various processes during simulation. The results of several simulation runs using different seed numbers are needed to reflect the average traffic conditions for a specific scenario. The method used to determine the number of required runs is explained as follows (Chu et al., 2004). First, five simulation runs are conducted; then, Equation (60), which specifies the required number of runs, is used to determine whether the five runs satisfy the criterion. If not, one additional run is conducted and then the required number of runs is calculated again. This process continues until the criterion is satisfied, at which point the current number of runs' results are averaged for performance analysis.

$$N = \left(t_{\alpha/2} \times \frac{\sigma}{\mu \times \varepsilon} \right)^2 \tag{60}$$

where

μ and σ = mean and standard deviation of a measure based on conducted simulation runs
ε = allowable error specified as a fraction of the mean μ
$t_{\alpha/2}$ = the critical value of the t - distribution at the significance levelα

In this study, $\varepsilon = 2\%$ and $\alpha = 0.05$.

The simulation results (with statistics) for the whole network under baseline control and adaptive control in all three scenarios are listed in Table 1. We found that five runs are sufficient for generating statistically meaningful results at the .05 significance level, with 2% allowable error for all four performance measures

Table 2 Performance of the network.

Variable	Average Travel Time (seconds)	Average Vehicle Speed (miles per hour)	Vehicle Mileage Traveled (miles)	Vehicle Hours Traveled (hours)
Scenario 1				
Baseline	344.3	43.9	760920.0	17367.6
Adaptive	331.0	45.9	762491.2	16725.5
Improvement (%)	3.9	4.6	0.2	3.7
Scenario 2				
Baseline	257.0	59.1	575585.6	9788.2
Adaptive	255.2	59.5	576046.1	9671.8
Improvement (%)	0.9	0.7	0.1	1.2
Scenario 3				
Baseline	249.5	60.9	382327.4	6284.3
Adaptive	248.4	61.1	382649.9	6263.4
Improvement (%)	0.5	0.3	0.0	0.3

in each scenario. The mean values of these measures, therefore, are used for further analysis.

Table 2 compares these measures of performance in all three scenarios. The corresponding improvements, which are represented as positive percentages, are also included. It is found that the network under adaptive control performs better than the baseline free-mode actuated control in all scenarios—drivers spend less time in the network and travel more distance with improved traveling speed. Specifically, Scenario 1 has gained the most improvement (i.e., 3.9% decrease in average travel time, 4.6% increase in average vehicle speed, 0.2% increase in vehicle mileage traveled, and 3.7% decrease in vehicle hours traveled), whereas Scenario 3 has gained the least improvement (i.e., 0.5% decrease in average travel time, 0.3% increase in average vehicle speed, 0.0% increase in vehicle mileage traveled, and 0.3% decrease in vehicle hours traveled). One possible reason underlying this result is that the low flow-level traffic may behave freely in the network without being affected by the change of control strategies.

A T-intersection is selected to demonstrate the performance of the proposed control model at the intersection level. This intersection corresponds to the junction of Irvine Center Drive and the offramp from southbound I-405, as shown in Figure 10. Phases 2 and 6 are assigned to the through movements and operate as min-recall phases, and Phase 4 is assigned to the left-turn movement without recall. The extension detectors (6 feet × 6 feet) for through phase are placed 300 feet upstream from the stop line, and the call and extension detectors (5 feet × 50 feet) for left-turn phase are placed right behind the stop line. The baseline control parameters for this signal are shown in Table 3.

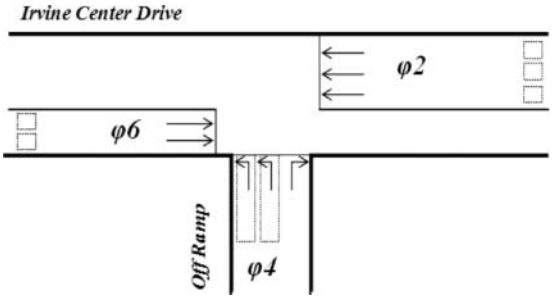

Figure 10 Study intersection.

For simplicity, only the simulation results from Scenario 1 are taken to evaluate the proposed control model at this T-intersection. Table 4 lists the simulation results (with statistics) over the whole 4-hr analysis period, which also indicates that five runs are sufficient and the mean values of performance measures can be used for analysis. Here, we take only the mean value of vehicle spillover as an example to illustrate the variation of measure of performance as the traffic condition changes. Figure 11 shows the identical flow profile under both baseline and adaptive controls for each signal phase as well as the entire intersection over the analysis period. These profiles are plotted with smoothed lines on the basis of the average flow data measured on 15-min intervals. As can be seen, Phases 2 and 4 experience two peak periods around 8 a.m. and 9 a.m., respectively, and Phase 6 experiences relatively steady and low level of flow. Accordingly, the total arrival flow for the entire intersection also experience two peak periods around 8 a.m. and 9 a.m.

Figure 12 illustrates the corresponding profiles of vehicle spillover under both baseline and adaptive controls for each signal phase and the entire intersection. Similarly, these profiles are plotted with smoothed lines based on the mean value over 15-min intervals. As can be seen, the vehicle spillover values are relatively high for Phases 2 and 4 around 8 a.m. and 9 a.m., respectively (and so is the total value for the entire intersection), whereas for Phase 6, it is constant at zero. This pattern is consistent with the flow profile as shown in Figure 11, which may infer that higher level of traffic flow causes more vehicle spillovers, and no vehicle spillover occurs at relatively low level of flow.

It can also be seen that the highest value of vehicle spillover in adaptive control, compared with that in baseline control,

Table 3 Parameters for the study intersection.

Phase (seconds)	2	4	6
Minimum green	8	5	8
Maximum green	40	24	40
Unit extension	5	2	5
Yellow and red	4	4	4

Table 4 Simulation results of the intersection (Scenario 1).

Variable	Vehicle Spillover (number)	Maximum Queue Length (feet)	Vehicle Travel Delay (seconds)
Baseline control			
M	48.0	160.2	1441.7
SD	1.2	4.7	42.5
Number of required runs	3.2	3.7	3.8
Adaptive control			
M	31.0	133.4	1211.1
SD	0.9	4.0	34.6
Number of required runs	3.7	3.8	3.7

decreases approximately by 1 for Phases 2 and 4 around the two peakperiods, respectively, and thus by 2 for the entire intersection. Also, the vehicle spillover number starts increasing from zero for Phases 2 and 4 (as well as the entire intersection) around 7:15 a.m. in baseline control, whereas it starts increasing later around 7:30 am in adaptive control. Therefore, it can be concluded that the adaptive control has the ability to reduce the number of vehicle spillover, especially during the period with high level of traffic flow.

The mean values of all three measures of performance under both baseline and adaptive controls over the whole simulation period are listed in Table 5. The corresponding improvements, which are represented as the difference in each measure of performance between baseline and adaptive control, are also included. The vehicle spillover in Phase 2 has been decreased by 9, and in Phase 4 has been decreased by 8. Probably because Phase 6 has relatively low flow rate, no spillover occurs in this phase for both controls. Some decreases in maximum queue length have been achieved with the improvement being 23.5 foot in Phase 2, 0 feet in Phase 4, and 3.3 foot in Phase 6. Although no improvement has been gained in the maximum queue length for Phase 4, the travel time for this phase has been reduced by 128.8 s. Also, the travel time is also reduced in Phase 2 by 84.1 s and Phase 6 by 17.7 s. The overall result shows the total improvement for the entire intersection in each measure of performance.

Simulation results show that the proposed control is promising. Even though the vehicle arrival pattern is assumed to be Poisson process in the model formulation, an assumption that may be violated in urban areas where intersections are closely spaced and/or high-level traffic flows are loaded, it can also be concluded that the proposed adaptive control model has the potential to improve the performance of the signalized network. Of course, better results would be expected were the real traffic flow pattern in urban networks to be modeled more accurately. Also, the control concept developed in this article may still be applied

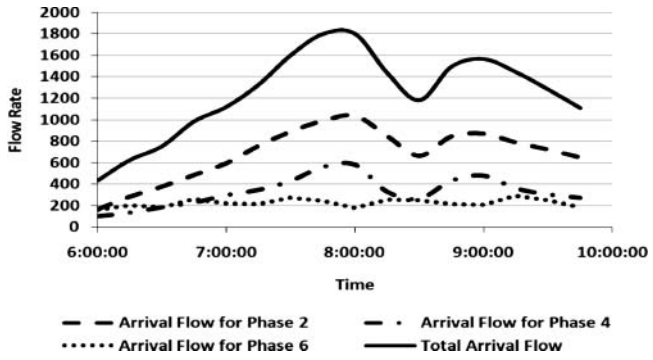

Figure 11 Flow profile at the study intersection.

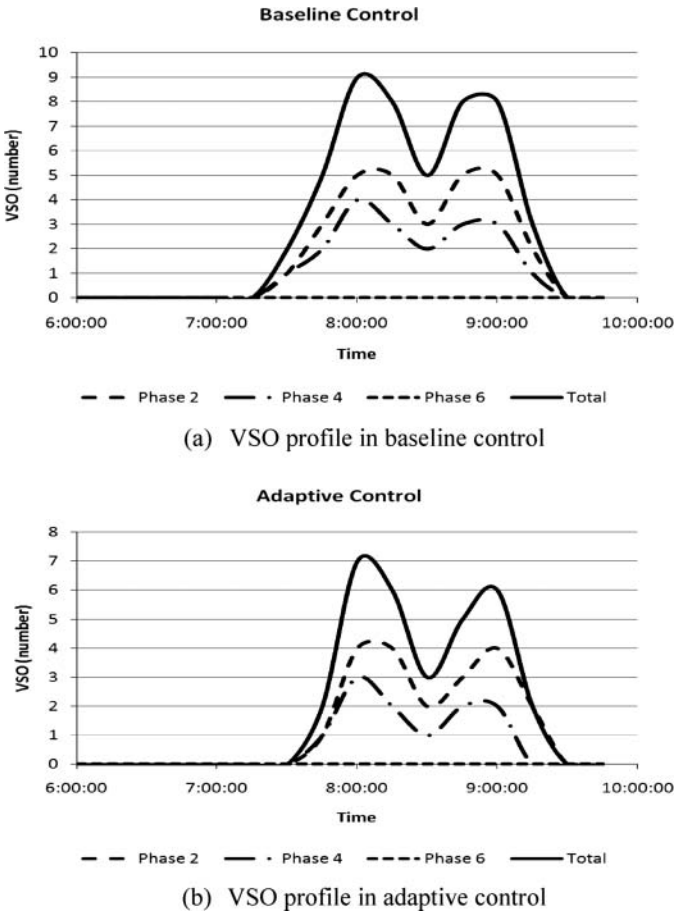

Figure 12 Vehicle spillover profile. (a) Vehicle spillover profile in baseline control. (b) Vehicle spillover profile in adaptive control.

Table 5 Performance of the intersection (Scenario 1).

Variable	Vehicle Spillover (number)	Maximum Queue Length (feet)	Vehicle Travel Delay (seconds)
Phase 2			
Baseline	29	77.1	683.4
Adaptive	20	53.6	599.3
Improvement	9	23.5	84.1
Phase 4			
Baseline	19	60.1	378.4
Adaptive	11	60.1	249.6
Improvement	8	0.0	128.8
Phase 6			
Baseline	0	23.0	379.9
Adaptive	0	19.7	362.2
Improvement	0	3.3	17.7
Overall			
Baseline	48	160.2	1441.7
Adaptive	31	133.4	1211.1
Improvement	17	26.8	230.6

via replacing the Poisson-related arrival pattern by, for example, the well-known Robertson's dispersion model (Robertson, 1969), or an empirical distribution obtained from field observations.

CONCLUSION AND FUTURE WORK

This article introduces a real-time adaptive signal control model that can be applied to an existing traffic-actuated control system to improve the performance of the signalized network. In this model, available signal-timing data, such as the max-out/gap-out information, parameter settings, and phase split, are fully used to describe the current and expected traffic conditions. Optimal control parameters are determined on the basis of these descriptions and provide signal-timing data for further optimizations. In formulating this adaptive control model, we restrict our focus on the basic control parameters that can be found in modern actuated controllers, hoping to ensure that the procedure developed here can be implemented with minimum adaption of existing field devices and the operating software.

We used microscopic simulation to test and evaluate the performance of the proposed control model in a calibrated network. Simulation results indicate that this model has the potential to improve the network performance under different traffic conditions. Future efforts will be made to improve this model by doing the following: (a) seeking a more sophisticated algorithm that considers platoon and dispersion factors to model the vehicle arrival pattern in signalized network, (b) further developing this model for the application to congested traffic conditions and coordinated-actuated signal control systems, and (c) programming other adaptive control strategies to compare with this model in simulation.

REFERENCES

Cameron, G. D. B., and Duncan, G. I. D. (1996). Paramics—Parallel microscopic simulation of road traffic. *Journal of Supercomputing*, **10**(1), 25–53.

Chou, Y. (1970). *Statistical analysis.* New York: Holt, Rinehart and Winston.

Chu, L., Liu, X., and Recker, W. (2004). Using microscopic simulation to evaluate potential intelligent transportation system strategies under nonrecurrent congestion. *Transportation Research Record,* **1886**, 76–84.

Darroch, J. N. (1964). On the traffic light queue. *Annals Math Statistics*, **35**, 380–388.

Head, K. L. (1995). An event-based short-term traffic flow prediction model. *Transportation Research Record*, **1510**, 45–52.

Hunt, P. B., Robertson, D. I., Bretherton, R. D., and Winton, R. I. (1981). SCOOT—A traffic responsive method of coordinating signals, Rep. LR1014. Transport and Road Research Laboratory, Crowthorne, England.

Kleinrock, L. (1975). *Queueing systems* (Vol. 1). New York: Wiley.

Lin, W., and Wang, C. (2004). An enhanced 0–1 mixed-integer LP formulation for traffic signal control. *IEEE Transactions on Intelligent Transportation Systems,* **5**, 238–245.

Liu, H., Sun, J., and Recker, W. (2005, January). *Dynamic date-driven short-term traffic flow prediction model for signalized intersections.* Poster presented at the 85th Transportation Research Board Annual Meeting, National Research Council, Washington, DC.

Lowrie, P. R. (1992). *SCATS: A traffic responsive method of controlling urban traffic control*. Technical Report, Roads and Traffic Authority, NSW, Australia.

McNeil, D. R. (1968). A solution to the fixed-cycle traffic light problem for compound poisson arrivals. *Journal of Applied Probability,* **5**, 624–635.

Mirchandani, P. B., and Head, K. L. (2001). A real-time traffic control system: Architecture, algorithms, and analysis. *Transportation Research Part C,* **9**, 415–432.

Robertson, D. I. (1969). TRANSYT: A traffic network study tool. RRL Report, No. LR253, Transport and Road Research Laboratory, Growthorne, UK.

Robertson, D. I., and Bretherton, R. D. (1991). Optimizing networks of traffic signals in real time-the scoot method. *IEEE Transactions on Vehicular Technology,* **40**(1), 11–15.

Sims, A. G. and Dobinson, K. W. (1980). The Sydney Coordinated Adaptive Traffic (SCAT) System Philosophy and Benefits. *IEEE Transactions on Vehicular Technology,* **29**, 130–137.

Transportation Research Board (TRB). (2000). *Highway Capacity Manual: Special Report 209.* Washington, DC: National Research Council.

Webster, F. (1958). *Traffic signal settings.* Road Research Technical Paper No. 56, Road Research Laboratory, London, England.

Wong, C. K., and Wong, S. C. (2003). Lane-based optimization of signal timings for isolated junctions. *Transportation Research Part B,* **37**, 63–84.

APPENDIX: NOTATIONS

λ	arrival flow rate
β	unit extension
g_e	effective green time
r_e	effective red time
q	departure flow rate
R	red duration time
G	phase split
G_q	queue service time
G_e	green extension period
Q	initial queue
Q^{spill}	vehicle spillover
$N(G_q)$	vehicle departure number in queue service time
$N(G_e)$	vehicle departure number in green extension period
$N(G)$	vehicle departure number in phase split
$G_{\min}$	minimum green
$G_{\max}$	maximum green
C	cycle length
$C_{\max}$	maximum allowable cycle length
TF	turning fraction
W	intersection control delay
S	saturation flow rate
l_1	startup lost time
l_2	clearance lost time
L	total lost time, equal to $(l_1 + l_2)$